Oleksandra Novosylna, Annette Doyle, Dmytro Vlasenko, Mark Murphy, Boris Negrutskii* and Anna El'skaya

# Comparison of the ability of mammalian eEF1A1 and its oncogenic variant eEF1A2 to interact with actin and calmodulin

DOI 10.1515/hsz-2016-0172
Received April 13, 2016; accepted July 26, 2016; previously published online August 2, 2016

**Abstract:** The question as to why a protein exerts oncogenic properties is answered mainly by well-established ideas that these proteins interfere with cellular signaling pathways. However, the knowledge about structural and functional peculiarities of the oncoproteins causing these effects is far from comprehensive. The 97.5% homologous tissue-specific A1 and A2 isoforms of mammalian translation elongation factor eEF1A represent an interesting model to study a difference between protein variants of a family that differ in oncogenic potential. We propose that the different oncogenic impact of A1 and A2 might be explained by differences in their ability to communicate with their respective cellular partners. Here we probed this hypothesis by studying the interaction of eEF1A with two known partners – calmodulin and actin. Indeed, an inability of the A2 isoform to interact with calmodulin is shown, while calmodulin is capable of binding A1 and interferes with its tRNA-binding and actin-bundling activities *in vitro*. Both A1 and A2 variants revealed actin-bundling activity; however, the form of bundles formed in the presence of A1 or A2 was distinctly different. Thus, a potential inability of A2 to be controlled by $Ca^{2+}$-mediated regulatory systems is revealed.

**Keywords:** actin bundling; calmodulin; higher eukaryotic elongation factors; protein-protein interaction.

***Corresponding author: Boris Negrutskii,** Laboratory of Protein Biosynthesis, Institute of Molecular Biology and Genetics, 150 Acad. Zabolotnogo Str., Kiev 03680, Ukraine, e-mail: negrutskii@imbg.org.ua
**Oleksandra Novosylna, Dmytro Vlasenko and Anna El'skaya:** Laboratory of Protein Biosynthesis, Institute of Molecular Biology and Genetics, 150 Acad. Zabolotnogo Str., Kiev 03680, Ukraine
**Annette Doyle and Mark Murphy:** General Engineering Research Institute, Liverpool John Moore University, Byrom Street, Liverpool L3 3AF, UK

## Introduction

Translation elongation factor eEF1A plays a main role in ribosomal polypeptide synthesis while providing the delivery of aminoacyl-tRNAs to the ribosome A-site (Negrutskii and El'skaya, 1998; El'skaya et al., 2013). This protein has also been shown to be multifunctional and is known to be involved in a number of non-translational cellular processes (Ejiri, 2002; Lamberti et al., 2004; Abbas et al., 2015). Within mammalian cells there exist two isoforms of translation elongation factor that share 97.5% homology: eEF1A1 (A1) and eEF1A2 (A2). The expression of the isoforms is tissue-specific (A2 is found in muscular, myocardial and neuronal tissue and in some specialized cells of pancreatic islet and gut) and mutually exclusive (Knudsen et al., 1993; Newbery et al., 2007); however, occasionally A2 appears also in the tissues where it is not expressed on a regular basis and this is thought to be related to tumor development (Anand et al., 2002; Tomlinson et al., 2005; Lee and Surh, 2009; Vislovukh et al., 2013; Xu et al., 2013; Kawamura et al., 2014; Sun et al., 2014; Yang et al., 2015). On the contrary, A1 is an ubiquitously and constitutively expressed protein that is not oncogenic *per se*, despite the fact that its expression may be de-regulated in transformed cells and tissues (de Wit et al., 2002; Mohler et al., 2002; Xie et al., 2002, also see for review Scaggiante and Bosutti, 2015).

The mechanisms of oncogenic action of the A2 isoform is mostly unknown, however, it is thought that A2 is involved in actin remodeling and enhanced cell migration and invasiveness in cancer cells (Amiri et al., 2007). The apparent difference in the abilities of the two isoforms to interplay with cellular partners may be among main reasons of their different oncogenic impact.

Previous studies have shown that both the A1 and A2 isoforms exhibit variations in their spatial molecular organization (Novosylna et al., 2007; Kanibolotsky et al., 2008), surface hydrophobicity and ability to form dimers (Timchenko et al., 2013) while the translational functions

of the A1 and A2 isoforms *in vitro* have been shown to be similar (Knudsen et al., 1993; Timchenko et al., 2013). Consequently, one may suggest that structural differences between the two isoforms may explain the observed differences in the ability of the isoforms to interact with different non-translational protein partners. In this context, it may be useful to compare the ability of the two isoforms to bind two known partners of eEF1A, namely actin and calmodulin, and estimate the consequences of possible differences.

eEF1A of different origin is known to bind calmodulin in a $Ca^{2+}$-dependent manner (Durso and Cyr, 1994; Kaur and Ruben, 1994; Kurasawa et al., 1996; Sengprasert et al., 2015). Moreover, calmodulin binding can interfere with eEF1A-mediated effects on cytoskeleton rearrangements (Durso and Cyr, 1994; Moore et al., 1998; Morita et al., 2008).

Also, eEF1A has been shown to bind and bundle actin filaments *in vitro* and enhance actin polymerization (Gross and Kinzy, 2005; Morita et al., 2008; Doyle et al., 2011). The overexpression of eEF1A in yeast has been found to result in a slow growth phenotype and altered actin cytoskeleton organization in the absence of any measurable effects on protein synthesis (Gross and Kinzy, 2005). Recently, the A1 isoform of mammalian eEF1A was shown to bind and bundle actin, supposedly due to a dimer formation (Vlasenko et al., 2015). In contrast, no information on the ability of A2 to interact with actin is currently available.

Here we show that the oncogenic and tissue specific A2 isoform did not bind $Ca^{2+}$-calmodulin. On the contrary, the A1 isoform readily interacted with $Ca^{2+}$-calmodulin *in vitro*. Moreover, endogenous calmodulin was precipitated by A1 from HEK293 cells. The domains of A1 involved into the interaction with $Ca^{2+}$-calmodulin were predicted by calmodulin target database (Yap et al., 2000) and confirmed experimentally. Functionally, $Ca^{2+}$-calmodulin displaced tRNA from the complex with A1 and inhibited actin-bundling activity of the latter, which indicated a multipotent role of the calmodulin-mediated regulation of A1. We hypothesize that the exclusive expression of A2 in muscle, myocardium and neuronal tissues may be explained by the need to prevent the translation process from being exposed to quick changes in $[Ca^{2+}]$ observed in these tissues. Importantly, A1 and A2 induced the formation of actin bundles displaying distinctly different form. Thus, one cannot exclude the existence of an A2-specific effect on F-actin bundling in cancer tissues contributing to the tumor-specific actin cytoskeleton disorganization.

# Results

## Only isoform A1 interacts with $Ca^{2+}$-calmodulin *in vitro*

Horizontal bidirectional polyacrylamide gel electrophoresis under non-denaturing conditions was used for the electrophoretic mobility shift assay (EMSA) (Novosylna et al., 2015). This method proved to be quite convenient and informative due to a significant difference in the molecular mass and the opposite surface charges of eEF1A and calmodulin. The eEF1A isoforms (~50 kDa) have an isoelectric point about 9.0 and move towards the cathode, while calmodulin (17 kDa) has a pI of 4.0 and moves toward the anode. The eEF1A isoforms (2.8 μM) were titrated with increasing amounts of $Ca^{2+}$-calmodulin. The complex of A1 and $Ca^{2+}$-calmodulin started to form at a 1:3 ratio (mol/mol) (Figure 1A, lanes 1–4) while an analogous complex of A2 was not detected even at 30-fold molar excess of $Ca^{2+}$-calmodulin (Figure 1A, lanes 5–8). Thus, there is a direct interaction of $Ca^{2+}$-calmodulin with the A1 rather than A2 isoform.

The Ni-NTA pull down assay was performed to examine the possibility of interaction of endogenous calmodulin with stably expressing A1-His in HEK293 cells. Importantly, this interaction was observed only in the presence of $CaCl_2$ while the addition of EGTA completely abolished the complex formation (Figure 1B). Also, endogenous eEF1A1 and calmodulin were found to be co-localized in HEK293 cells (Supplementary material Figure S1).

## Identification of calmodulin-binding sites in eEF1A1

To approach an explanation as to why the highly similar isoforms show a cardinally different ability to bind $Ca^{2+}$-calmodulin, the amino acid sequences of the proteins were analyzed using the calmodulin target database (Yap et al., 2000). Indeed, a noticeable difference between the isoforms was found, namely the A1 isoform contained an extended calmodulin binding site, comprising two binding regions located in domain II (residues 311–327) and domain III (residues 422–437). These regions are referred to as calmodulin binding site of domain II (CBSDII) and calmodulin binding site of domain III (CBSDIII). No CBSDII and only a shortened version of CBSDIII (residues 427–438) were predicted in the A2 molecule (Figure 2A). This could explain the observed

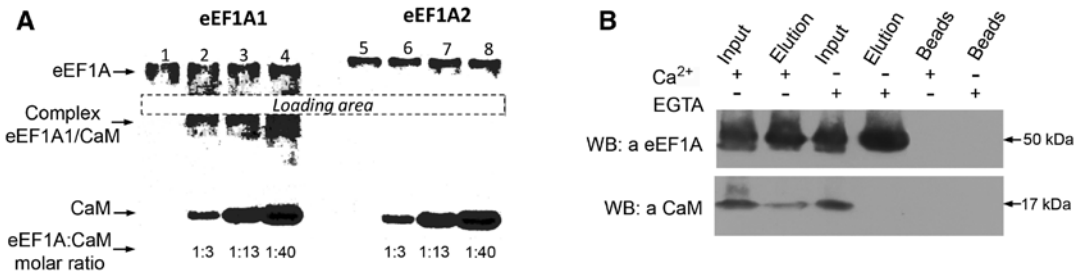


**Figure 1:** eEF1A1-calmodulin complex formation.
(A) Non-denaturing polyacrylamide gel (7%) stained with Coomassie Brilliant Blue shows the complex of A1 with calmodulin and lack of such complex with A2. 2.8 μM eEF1A was mixed with 8 μM, 36 μM or 109 μM calmodulin in buffer containing 30 mM Tris, pH 7.5, 20% glycerol, 1 mM $MgCl_2$ and 6 mM 2-mercaptoethanol. Lanes: 1 – A1 alone; 2 – A1 and calmodulin (molar ratio 1:3); 3 – A1 and calmodulin (molar ratio 1:13); 4 – A1 and calmodulin (molar ratio 1:40); 5 – A2 alone; 6 – A2 and calmodulin (molar ratio 1:3); 7 – A2 and calmodulin (molar ratio 1:13); 8 – A2 and calmodulin (molar ratio 1:40). The eEF1A variants migrate towards the cathode (top of the gel) while calmodulin and the eEF1A-calmodulin complex migrate towards the anode (bottom of the gel). (B) A1 and calmodulin form the complex in the calcium dependent manner. The complex of His-tagged A1 and calmodulin was precipitated from HEK293 cell line stably expressing A1-His, using NiNTA resin. The resin was washed extensively, and then bound proteins were eluted by boiling in the Laemmli sample buffer. Samples were resolved by SDS-PAGE and visualized by immunoblotting with corresponding antibodies. One millimolar $CaCl_2$ or 1 mM EGTA was added at every step of the assay. Non-transfected HEK293 lysates were used as control for non-specific binding to Ni-NTA resin (last two lines). Input – lysate of the same cells made in the presence of 1 mM $CaCl_2$ or EGTA as indicated.

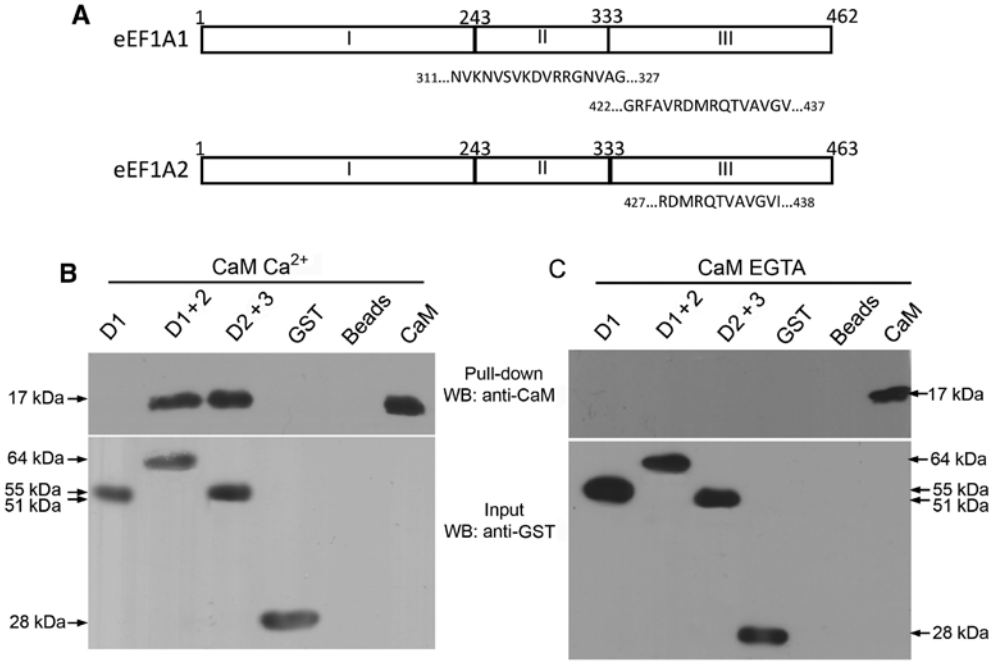


**Figure 2:** Identification of calmodulin-binding sites.
(A) Schematic representation of the A1 and A2 structures. Three known domains of eEF1A are marked I, II and III. The sequences of the predicted calmodulin interaction sites calculated by calmodulin target database engine, are indicated. (B) Binding of calmodulin to different domains of A1. Different GST-fused constructs coupled with glutathione sepharose beads were incubated with calmodulin, washed and eluted with 20 mM glutathione. Assays were performed in the buffer containing 1 mM $CaCl_2$ (left panel) or 1 mM EGTA (right panel). D1 – domain 1 (1–243, 55 kDa), D1+2 – domain 1+domain 2 (1–333, 64 kDa), D2+3 – domain 2+domain 3 (244–462, 51 kDa). CaM – calmodulin control.

difference between the interaction and non-interaction of A1 and A2 with calmodulin.

The location of the calmodulin-binding regions in A1 was investigated experimentally using a pull-down assay with the GST-fusion constructs comprising domain I, domain (I+II) and domain (II+III) of A1 (Vlasenko et al., 2015). Domain II and probably domain III of eEF1A1 were shown to bind calmodulin, which correlated well with

the bioinformatics prediction. This interaction was $Ca^{2+}$-dependent (Figure 2B, left panel), as the presence of EGTA precluded the complex formation (Figure 2B, right panel).

## Modeling of the A1-$Ca^{2+}$-calmodulin complex

As both bioinformatic and experimental data supported the involvement of CBSDII and CBSDIII in the interaction of A1 with calmodulin, these epitopes were selected during the calmodulin receptor formatting for the molecular docking. A1 was modeled by taking recently solved A2 crystal structure (Crepin et al., 2014) as a template. It should be noted that spatial structures of A1 and A2 in individual state, their hydrophobicity and ability to form dimers, may be different (Novosylna et al., 2007; Kanibolotsky et al., 2008; Timchenko et al., 2013). A1 shows an extended conformation while A2 is a compact protein (Novosylna et al., 2007; Kanibolotsky et al., 2008). However, it is known that «extended» proteins, including A1, adopt a compact conformation upon interaction with a ligand (Budkevich et al., 2002; Shiau et al., 2006). That is why we believe the compact X-ray structure of eEF1A2 may be used as an approximation to model the compact structure of eEF1A1 in the complex with calmodulin. As mentioned above, the minor amino acid substitutions in the CBSDII and CBSDIII sequences could be responsible for the apparent inability of A2 to interact with calmodulin.

The complex of IQCG (IQ Motif Containing G) protein and $Ca^{2+}$-bound calmodulin (PDB ID:4M1L) was chosen as a reference structure for the A1 docking to calmodulin. The A1 model orientation was configured to be static, whereas the calmodulin molecule allowed rotating. Visual examination discovered a number of analogous complexes that could be divided into several groups: in the main groups A and B, the complexes approximated to the predictions from the bioinformatics studies. Group A showed one calmodulin molecule attached to both predicted binding sites in the eEF1A1*GDP molecule. A representative model (complex #32) is shown in Figure 3A. In this complex, residues 315–323 created an interface between domain II of the A1 model and the C-terminal 'hand' of calmodulin, which correlates well with the bioinformatics prediction of CBSDII (Figure 2A) and earlier molecular dynamic simulation estimate (Kanibolotsky et al., 2008). The bioinformatics prediction of CBSDIII also correlates with the docking model. The three residues (430-RQT-432) which are situated in the middle of CBSDIII create contacts with the opposite 'hand' of the calmodulin molecule. Importantly, the residues flanking the 430-RQT-432 region of CBSDIII do not appear to be exposed; being either covered by the Helix B of domain I or buried in domain III (like Phe424 and Val426). Some additional interacting clusters can be found in domain I, one of which is located near the conserved Thr72 residue from the SWITCH I region (Arg69 and Ile71). However, these contacts are probably rather weak as they are not important for the structural interaction (Figure 2B). The amount of residues that take part in the interface formation is 27 for eEF1A1 and 28 for calmodulin. The area of the interaction interface is 812.6 $Å^2$. The degree of the interaction specificity ($p$-value) is 0.469, indicating that $\Delta^iG$ value is typical for this type of interface. We termed this model as the A1 mode of calmodulin binding.

Group B, representing nearly 25% of the complexes predicted by the docking, comprised the models where the calmodulin molecule was attached exclusively to the region of CBSDIII. In this case, one of the calmodulin 'hand' domains is bound while another is free. A representative model (complex #17) is shown in Figure 3B. This model is not supported by experimental data for eEF1A1, but it is of interest as it may correspond to hypothetic A2-like way of binding, as according to calmodulin target database, A2 may have a single and reduced calmodulin-binding site in domain III (Figure 2A).

As the A1 and A2 molecules can exist in dimeric form (Timchenko et al., 2013; Crepin et al., 2014) and the dimers were suggested to be of functional importance (Bunai et al., 2006; Migliaccio et al., 2015; Vlasenko et al., 2015) it was estimated whether calmodulin binding in the A1 or A2 mode can interfere with the dimer formation (Figure 3C). Interestingly, CBSDIII is buried inside the dimer, so in this case the interaction of calmodulin with this site seems impossible. Consequently, it may prevent the interaction of the A2 dimer with calmodulin, as CBSDIII is the only interaction site predicted for A2. At the same time, CBSDII, present exclusively in the A1 structure, remains totally exposed in the dimer. Thus, it is possible, that in the A1 dimer one 'hand' of the calmodulin molecule binds to CBSDII first, and then dissociation of the dimer is induced, which makes CBSDIII exposed and available for binding by another 'hand' of the calmodulin molecule.

## Calmodulin interferes with tRNA-binding activity of eEF1A1

One of the ways calmodulin interferes with cellular processes is through its direct binding to target proteins. As there is an obvious difference between the A1 and oncogenic A2 isoforms in their ability to bind $Ca^{2+}$-calmodulin,

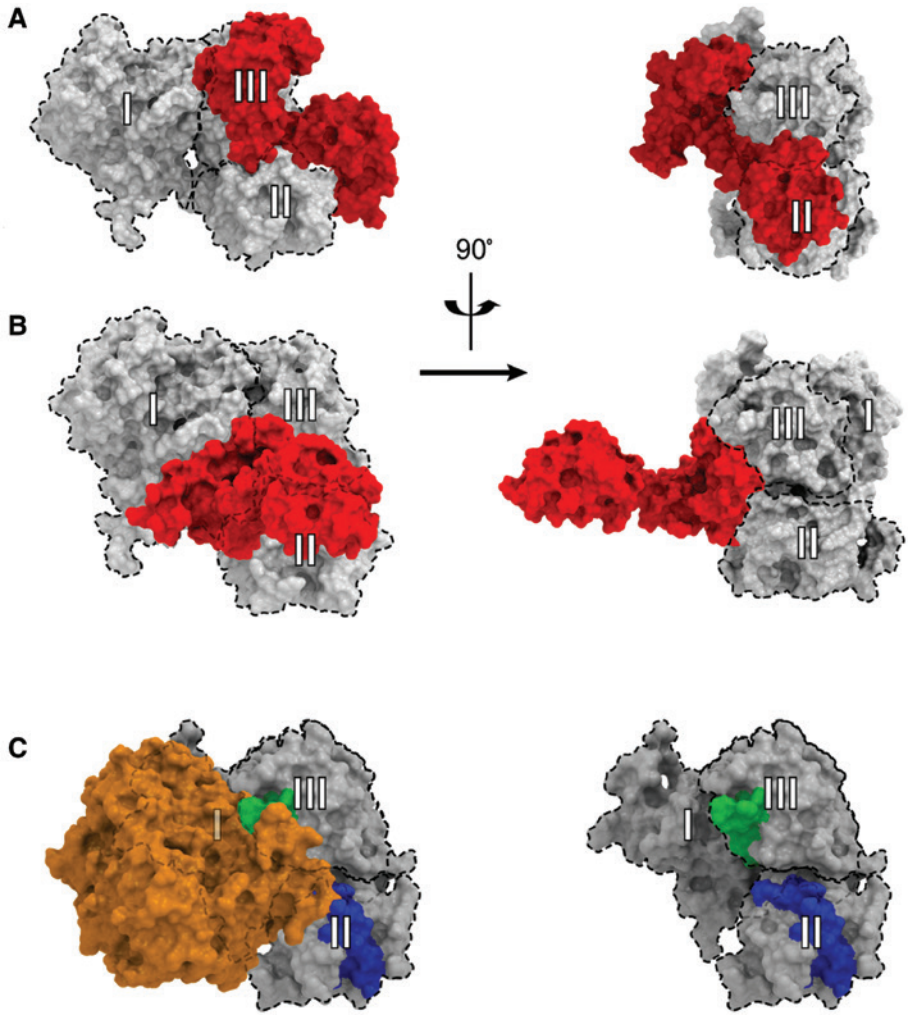


**Figure 3:** Possible interaction modes of the A1 or A2 isoforms with $Ca^{2+}$-calmodulin.
(A) The eEF1A1-calmodulin complex interaction model with calmodulin bound to both predicted sites within domains II and III. eEF1A1 is in grey and its domains are labeled. Calmodulin is in red. (B) The eEF1A2 interaction model with calmodulin bound to only one predicted site within domain III with one 'head' on a loose. eEF1A2 is in grey and its domains are labeled. Calmodulin is in red. (C) CBSDII rather than CBSDIII is exposed in the dimeric structure of eEF1A. On the left is dimer, on the right is monomer. In the dimer, one eEF1A molecule is colored grey and another is colored brown. CBSDII is in blue, CBSDIII is in green.

it is important to estimate a potential functional role of the specific A1-calmodulin interaction. First, we assessed the potential of calmodulin to interfere with translation elongation catalyzed by A1. As the location of the predicted calmodulin-binding site of A1 gained experimental support, it appeared important to estimate how it may overlap with the A1 sites of interaction with translational partners like tRNA. These interaction sites were deduced from the crystal structures of the corresponding complexes (PDB ID: 1b23, 1F60) (Nissen et al., 1999; Andersen et al., 2000; Soares et al., 2009). Indeed, an overlap of the calmodulin and tRNA interaction sites in the A1 molecule was found (Figure 4A). To examine experimentally, whether this apparent overlap in binding sites results in competition between calmodulin and tRNA, the complex of A1 with [$^{32}$P]-$tRNA^{Leu}$ was formed and titrated with increasing concentrations of $Ca^{2+}$-calmodulin (Figure 4B). EMSA in native gel was used to follow the reaction course. A1 and tRNA form a strong complex that does not enter native gel, therefore it is not visible on the autoradiograph. In this case, only a small amount of free tRNA is seen (Figure 4B, upper panel, lane 5). Upon addition of calmodulin, the intensity of the bands corresponding to free tRNA increases sharply, indicating that calmodulin ousts tRNA from the complex with A1. This can be observed at equimolar calmodulin: A1 ratio (Figure 4B, upper panel, lanes

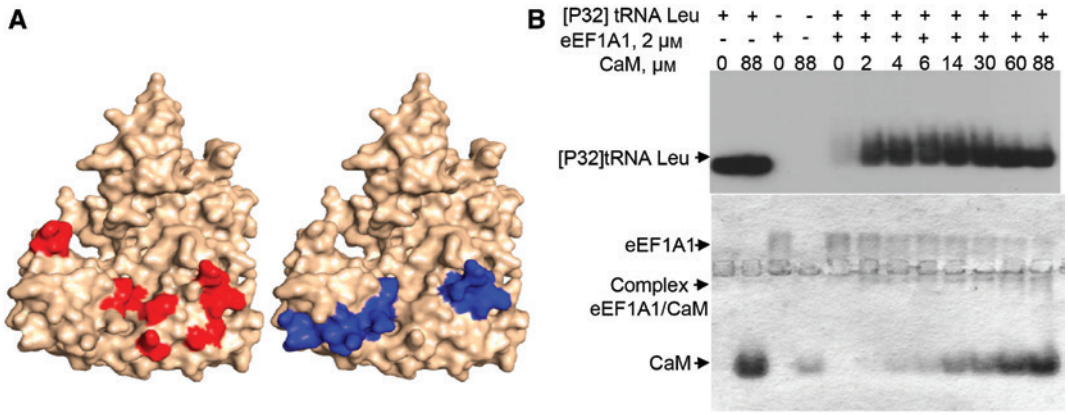


**Figure 4:** Calmodulin can interfere with translation function of A1.
(A) The tRNA and calmodulin binding sites in eEF1A partially overlap. The location of the tRNA-binding site (left panel) marked red and calmodulin-binding site (right panel) marked blue is shown in the yeast eEF1A crystal structure (PDB ID: 1F60). (B) Calmodulin ousts [$^{32}$P]-tRNA$^{Leu}$ from the complex with A1. Upper panel: autoradiograph of the gel. Bottom panel: gel shift assay of A1, calmodulin and radiolabeled tRNA$^{Leu}$. Coomassie Brilliant Blue staining.

6–12). The interaction of calmodulin with A1 is reflected by the inverse relationships between the calmodulin concentration rise and the decreasing A1 band intensity (Figure 4B, bottom panel, lanes 6–12**)**. Thus, a competition between calmodulin and tRNA for A1 is possible and this may interfere with the translational activity of the latter.

We were also interested to determine whether the presence of calmodulin would affect the ability of A1 to bind guanine nucleotide (Supplementary material Figure S2). The presence of calmodulin (even at 10-fold excess) had no effect on spontaneous GDP exchange in the A1 molecule. This data correlates with the lack of interaction between nucleotide binding of domain D1 and calmodulin, which was shown both experimentally and through bioinformatics studies.

## A1 and A2 generate actin bundles that have different morphology

Another established binding partner of eEF1A is actin. The comparison of the A1 and oncogenic A2 interaction with F-actin is of importance, as the changes in the regulation of the cytoskeleton are often involved in cancer development and metastatic transformation (Rao and Li, 2004; Amiri et al., 2007; Mouneimne et al., 2012; Fife et al., 2014). To examine possible differences in the actin bundling capabilities of A1 and A2, atomic force and confocal microscopy were carried out. Results showed a pronounced effect of both isoforms on the formation of F-actin bundles (Figure 5A and B). For AFM, similar results were obtained using different substrates including mica (Figure 5A) and graphite (data not shown).

Contrary to A1, short, thick, splinter-like bundles were formed in the presence of the oncogenic A2 isoform (Figure 5B). As the formation of actin bundles is most probably triggered by the dimers of eEF1A (Vlasenko et al., 2015), the difference in the appearance of actin bundles may be explained by the recent finding that the A2 dimers are essentially more compact than that of A1 (Timchenko et al., 2013).

## Calmodulin negatively influences actin-bundling activity of A1

As $Ca^{2+}$-calmodulin was reported to inhibit sea urchin and Tetrahymena eEF1A-catalyzed actin bundling (Morita et al., 2008; Fujimoto and Mabuchi, 2010), we used this model to examine the ability of calmodulin to interfere with actin bundling induced by mammalian A1. Figure 5C shows that $Ca^{2+}$-calmodulin negatively influenced actin bundling by A1, suggesting an impact of $Ca^{2+}$-calmodulin on the non-translational functions of A1.

It should be noted that some inhibitory effect of $Ca^{2+}$-calmodulin on the A2-induced actin bundling *in vitro* was also observed (data not shown). The reasons for this remain unclear, as calmodulin does not interact with A2 (Figure 1A) and actin (data not shown) *in vitro*. As mentioned above, the existence of some calmodulin binding site was predicted in domain III of A2 (Figure 2A and B). As domain III of eEF1A is also responsible for actin binding (Vlasenko et al., 2015) some competition may exist between calmodulin and actin for monomeric A2 and this may explain this result. However, as shown

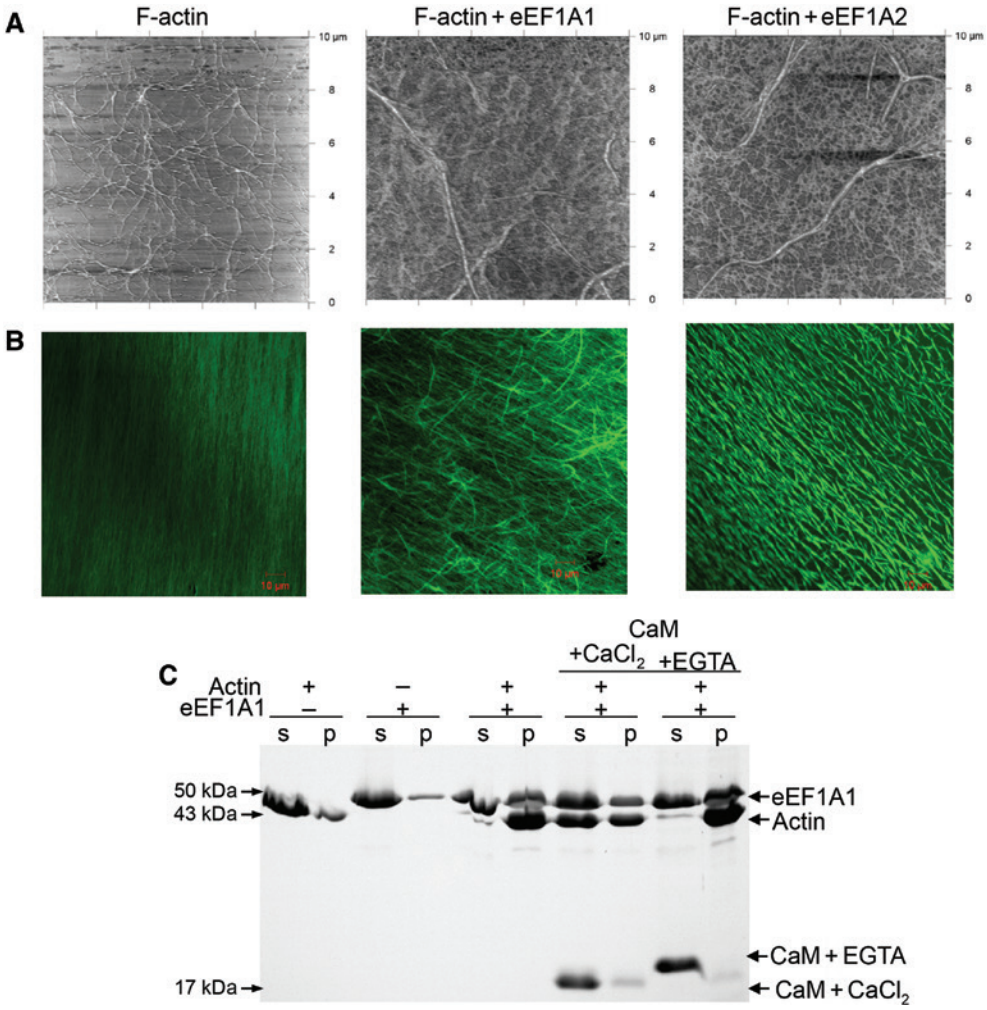


**Figure 5:** Actin-bundling activity of the eEF1A isoforms.
(A) AFM tapping mode image of F-actin stabilized with phalloidin (left panel), F-actin bundled in the presence of A1 (central panel) or A2 (right panel). Height image, mica substrate. (B) Confocal microscope images of F-actin: phalloidin-stabilized F-actin filaments (left panel), F-actin bundling in the presence of A1 (central panel) or A2 (right panel). All images were captured using a 63× oil immersion lens. (C) Effect of calmodulin on the actin bundle formation induced by A1. Low-speed actin co-sedimentation assay. Nine micromolar actin was prepared as described in Materials and Methods and mixed with 9 μM A1 and 13 μM calmodulin in the presence of 1 mM $CaCl_2$ or 1 mM EGTA. The supernatants (S) and pellets (P) were analysed by SDS-PAGE stained with Coomassie Brilliant Blue. The bands corresponding to A1, actin and calmodulin are shown by arrows.

in Figure 1A, the extended and potent calmodulin binding site of eEF1A1 provides much more efficient binding of the ligand than the severely reduced analogous site in the A2 molecule.

Thus, one may suggest a potential role of calmodulin in both translation and non-translational functions of A1 rather than A2.

## Discussion

The intriguing tumor-inducing appearance of the A2 variant of translation elongation factor 1 in ovary cancer was detected over a decade ago (Anand et al., 2002). Since then, the A2 isoform has been found in a number of different human cancer tissues and evidence for its oncogenic role obtained (Abbas et al., 2015). Recently, it was found that the induction of non-specific expression of A2 in tumors might result from the loss of microRNA-mediated control (Vislovukh et al., 2013). The 97.5% homologous A1 and A2 isoforms were described to possess different shapes in solution, different hydrophobic properties and ability to form dimers (Timchenko et al., 2013). X-ray structure of eEF1A2*GDP was recently published (Crepin et al., 2014) while the A1 isoform could not be crystallized, supposedly due to its 'extended' conformation

(Budkevich et al., 2002). The question as to why A2 revealed oncogenic properties still remains unanswered.

We reason that differences in the structural properties of the isoforms might provide a basis for their different interactions with protein partners, including those involved in signaling and maintaining cell shape, which, in turn, might contribute to oncogenesis. To investigate this possibility in principle, we used two known protein partners of eEF1A, calmodulin and actin. Intriguingly, the oncogenic A2 isoform has revealed much less ability to bind calmodulin as compared to A1. In line with that, our preliminary studies suggest that contrary to A1, A2 does not bind S100A6, which is a disparate member of the family of $Ca^{2+}$-related proteins (Novosylna, Filipek and Negrutskii, unpublished observation). Recent data reported the inability of A2 rather than A1 to form a complex with co-chaperone Sgt1, which plays a role in cell division (Novosylna et al., 2015). On the other side, A2 showed increased, as compared to A1, ability to interact with SH2 and SH3 domains of different signaling molecules *in vitro* (Panasyuk et al., 2008). However, the analysis of published phosphoproteomics data suggested that the tyrosine residues, which are readily phosphorylated in A1, are not modified in the A2 isoform in cancer tissues (Negrutskii et al., 2012).

Thus, our own data and that reported within the literature lead us to assume that the A2 isoform may be less important (compared to A1) for $Ca^{2+}$-modulated cellular control and which may make translation less prone to the conditions of permanent changes in $Ca^{2+}$ concentrations in muscle, myocardial and neuronal tissues, where A2 is expressed as the only eEF1A isoform (Knudsen et al., 1993; Lee et al., 1993). However, the expression of A2 can be sporadically induced in the tissues where the only A1 isoform is present normally (Anand et al., 2002; Lee, 2003; Li et al., 2006; Zhu et al., 2007; Cao et al., 2009; Lee and Surh, 2009; Vislovukh et al., 2013). In such tissues, newly appeared A2 can escape A1-adapted regulation and act in an uncontrolled way, thus acquiring oncogenic properties. Possible regulatory mechanisms involved will be a subject of further investigations. We believe that the actin-bundling role of A2 should be specially considered as cancer-related one, because the dysregulated actin bundling may play a key role in metastatic processes (Hashimoto et al., 2007; Stevenson et al., 2012).

A role of A1 under conditions of dysregulation of calmodulin amount or $Ca^{2+}$ flux in the cells could be also essential as these conditions may influence the amount of 'free' A1 protein, thus having an impact on its functionally important re-distribution to different translational and non-translational compartments (Sasikumar et al., 2012; Abbas et al., 2015).

A number of the paralogue protein families have been described recently, where one representative of a family was oncogenic while another was not (Kim et al., 2009; Lau et al., 2012; Huang et al., 2014; Samyesudhas et al., 2014; Sirianant et al., 2014). It is known that minimal changes in the amino acid sequence and/or post-translational modification status of a protein may lead to total rearrangement of its conformation and multimeric state (Alexander et al., 2007, 2009; Khan et al., 2013) which may be the case of eEF1A2. The paralogues may differ in post-translational modifications (Tossidou et al., 2012; Guo et al., 2015; Werner et al., 2015), reveal distinct tissue expression (Kim et al., 2009; Samyesudhas et al., 2014), cellular localization (Sirianant et al., 2014), and functions (Bai et al., 2011; Palmer et al., 2012; Wanitchakool et al., 2014; Fu et al., 2016). Unfortunately, fundamental basis for this metamorphosis, which could be a different ability of the variants to interact with diverse cellular partners (Jacobsen et al., 2010) remains mostly unexplored. Generalizing our data, one may suggest that in some cases, subtle changes in the amino acid sequences of 'oncovariant' paralogues make their conformation less suitable for interactions with cellular partners compared to their counterparts. Thus, cellular contacts of oncoproteins can be modified or even eliminated, as compared to normal paralogues. This effect may be caused by the substitution of amino acids directly involved in protein-ligand interactions, as well as the substitutions of amino acids, which are post-translationally modified in one of the variants.

## Materials and methods

### Materials

The eEF1A isoforms (more than 90% purity) was isolated from rabbit liver or muscles as described (Shalak et al., 1997; Lukash et al., 2004; Yaremchuk et al., 2012). The rabbit skeletal muscle actin was purchased from Cytoskeleton, Inc. (Denver, USA). The protein was reconstituted, according to the manufacturer's instructions. Before each experiment, actin was incubated on ice for 60 min followed by centrifugation at 16 000 *g* for 15 min. The plasmids coding for recombinant domains of *Homo sapiens* eEF1A1: D1 (1–243), D1 + D2 (1–333), D2 + D3 (244–462) were generously gifted by C. Knudsen. The domains were expressed as the GST-fusion proteins in *E. coli* and purified with glutathione sepharose 4B beads from GE Healthcare Life Sciences (Little Chalfont, UK) according to the manufacturer's instructions. [$P^{32}$]-labelled $tRNA^{Leu}$ was kindly gifted by Dr. Futernyk.

### Purification of calmodulin

All procedures, except high-temperature treatment and phenyl-sepharose chromatography, were carried out at +4°C. Cow brain (~350 g) was grinded and homogenized in two volumes of homogenization buffer [50 mM Tris-HCl pH 7.5, 2 mM 2-mercaptoethanol, 1 mM EDTA, 0.5 mM phenylmethylsulfonyl fluoride (PMSF)] for 1 min. Homogenate was centrifuged 40 min at 14 000 *g*. The supernatant was passed through four layers of cheesecloth. Then $(NH4)_2SO_4$ was added at constant stirring to 60% saturation (36.6 g/100 ml of the supernatant). pH of solution was adjusted to 4.1 with 6 M acetic acid. After formation of the precipitate for at least 2 h, the proteins were recovered by centrifugation for 30 min at 14 000 *g*. The pellet was dissolved in a minimal volume of buffer containing 50 mM Tris-HCl pH 7.5, 2 mM 2-mercaptoethanol. pH was adjusted to 7.5 with 1 M Tris solution and centrifuged again under the same conditions to remove insoluble proteins. The resulting supernatant was incubated in small portions (~30 ml) for 5 min in a boiling bath and cooled in ice. Heat denatured protein was removed by 60 min centrifugation at 2000 *g*. Chromatography on phenyl-sepharose was carried out at room temperature. One molar $CaCl_2$ was added to supernatant to a 5 mM final concentration and applied to phenyl sepharose CL-4B column, equilibrated with buffer containing 50 mM Tris-HCl pH 7.5, 2 mM 2-mercaptoethanol, 0.1 mM $CaCl_2$. Unbound proteins were washed out with the same buffer and then with the same buffer containing 0.5 M NaCl. Calmodulin was eluted with buffer containing 50 mM Tris-HCl pH 7.5, 2 mM 2-mercaptoethanol, 3 mM EGTA. Then, calmodulin was concentrated on Q-sepharose and dialyzed against buffer containing 25 mM Tris-HCl pH 7.5, 10% glycerol, 6 mM 2-mercaptoethanol.

### Electrophoretic mobility shift assay (EMSA)

Horizontal non-denaturing gel electrophoresis was carried out as described in Novosylna et al. (2015). Before running, the samples were incubated for 10 min at 37°C in the binding buffer containing 30 mM Tris-HCl, pH 7.5, 20% glycerol, 1 mM $MgCl_2$, 6 mM 2-mercaptoethanol and 1 mM $CaCl_2$. After electrophoresis, the gel was stained with Coomassie Brilliant Blue. In the experiments using radiolabeled tRNA, the gel was dried before autoradiograph was captured.

### SDS-PAGE and Western blotting

Gel electrophoresis in 15% (w/v) polyacrylamide containing 0.1% SDS (SDS-PAGE) was performed as described (Laemmli, 1970). Separated proteins were electrotransferred onto nitrocellulose membrane and identified using mouse monoclonal anti-eEF1A from Merck Millipore (Billerica, USA) diluted 1:5000, rabbit monoclonal anti-calmodulin from Novus Biologicals, (Cambridge, UK) diluted 1:5000 or mouse polyclonal anti-GST antibody (home-made, kindly provided by Dr. O. Gorbenko, IMBG, diluted 1:500). After washing with PBST (PBS plus 0.1% Tween-20) blots were incubated with secondary antibodies (goat anti-mouse HRP-conjugated antibody (1:10 000) from Amersham Biosciences (Amersham, UK), anti-rabbit HRP-conjugated antibody (1:10 000, Amersham Biosciences) and goat anti-mouse IgG antibodies conjugated to horseradish peroxidase (1:10 000) (Merck Millipore). Blots were developed with the ECL kit (Amersham Biosciences).

### His-tag pull-down assay

The protein lysates of HEK293 cells overexpressing eEF1A1-His were prepared in the lysis buffer containing 50 mM Tris-HCl pH 7.5, 100 mM NaCl, 10 mM imidazole and the cocktail of protease inhibitors from Roche (Basel, Switzerland). Then the lysates were centrifuged at 14 000 *g* for 20 min. The supernatant fractions were applied to the Ni-NTA resin equilibrated with the lysis buffer. The resin was incubated 1 h at 4°C with agitation and washed sequentially with wash buffer I (50 mM Tris-HCl pH 7.5, 300 mM NaCl, 10 mM imidazole) and wash buffer II (50 mM Tris-HCl pH 7.5, 500 mM NaCl, 20 mM imidazole). The carrier was equilibrated with binding buffer (50 mM Tris-HCl pH 7.5, 100 mM NaCl) supplemented with 1 mM $CaCl_2$ or 1 mM EGTA. The samples were incubated 1 h at 4°C with agitation and washed with the same buffer. Bound proteins were eluted with the SDS sample buffer and analyzed by SDS-PAGE.

### GST pull-down assay

Purified calmodulin was dialyzed against buffer containing 30 mM Tris-HCl, pH 7.5, 20% glycerol, 1 mM $MgCl_2$, 6 mM 2-mercaptoethanol) supplemented with 1 mM $CaCl_2$ or 1 mM EGTA and incubated with GST or GST-fusion domains of A1 bound to the glutathione beads. The Sepharose was washed with the the same buffer three times. Samples were eluted from the resin with the elution buffer (20 mM reduced glutathione, 50 mM Tris-Cl, pH 8.0). Calmodulin was detected with anti-calmodulin antibodies (Novus Biologicals).

### Actin-bundling assay

The effect of calmodulin on actin bundle formation was examined using the low-speed actin co-sedimentation assay as described previously (Vlasenko et al., 2015). A1 and calmodulin were dialyzed against buffer containing 30 mM Tris-HCl, pH 7.5, 20% glycerol, 1 mM $MgCl_2$, 6 mM 2-mercaptoethanol. Actin (9 μM) was prepared as described above and incubated with A1 (9 μM) and calmodulin (13 μM) in a total volume of 25 μl for 30 min at room temperature. The volume of each sample was adjusted with the same buffer. The mixture was supplemented with 50 mM KCl, 2 mM $MgCl_2$ and 1 mM ATP. The samples were centrifuged at 16 000 *g* for 15 min. The supernatants and pellets were solubilized in the SDS-PAGE sample buffer and analyzed by SDS-PAGE, with subsequent Coomassie Blue staining.

### Actin-bundling microscopy studies

**Atomic force microscopy:** Imaging of F-actin in the presence and absence of eEF1A was carried out using atomic force microscopy (AFM) as described previously by (Doyle et al., 2011). Briefly, actin was polymerized and eEF1A added in 5:1 actin: A1 or A2 ratio. Next, the actin:eEF1A was deposited onto mica or graphite substrates, left to air-dry at ambient temperature and imaged using atomic microscopy. AFM images were obtained using a Molecular Force Probe-3D (MFP-3D) atomic force microscope (Asylum Research, Goleta, USA) operated in AC mode using Olympus AC240 cantilevers.

**Confocal microscopy:** F-Actin was prepared as described above using a 5:1 actin:eEF1A1 or eEF1A2 ratio and labeled with Acti-stain 488 Phalloidin (Cytoskeleton Inc.) according to the manufacturer's instructions. All confocal microscopy images were captured with a Zeiss LSM510 confocal microscope. For imaging Phalloidin-labelled actin an argon-ion laser (488 nm excitation) was used. All images were captured using a 63× oil immersion lens.

### Computer modeling and docking procedures

eEF1A1 homology modeling was performed using MODELLER (Sali and Blundell, 1993) online service hosted by the UCSF RBVI. Crystal structure of mammalian eEF1A2 (PDB ID:4C0S) was used as a template. UCSF Chimera 1.10.2 (Pettersen et al., 2004) provided a graphical interface to running the program MODELLER online. Molecular docking was performed in Molsoft ICM Pro 3.8-3 software (Abagyan et al., 1994). The calculation algorithm is based on the all-atom vacuum force field ECEPP/3, taking into account solvation free energy and entropic contribution. Conformational sampling is based on the biased probability Monte Carlo (BPMC) procedure with random selection of a certain conformation in the internal coordinate space, with sequential shift to a new random position independent of the previous position but according to a predefined continuous probability distribution. For each state, additional full local minimization was performed. Rendering of images for illustrations was performed in UCSF Chimera 1.10.2. (Pettersen et al., 2004).

**Acknowledgments:** The authors are grateful to P. Futernyk for individual tRNA preparations, C.R. Knudsen for eEF1A1 domain constructs, S. Havrylenko for participation in initial experiments. We appreciate A. Horuzhenko's contribution to the confocal microscopy studies. Research was supported in part by the Scientific program of NASU 'Molecular and cell biotechnologies for medicine, industry and agriculture' and GDRI Program 'Human pathologies: from molecular to cellular level'.

## References

Abagyan, R., Totrov, M., and Kuznetsov, D. (1994). ICM-A new method for protein modeling and design: applications to docking and structure prediction from the distorted native conformation. Comput. Chem. *15*, 488–506.

Abbas, W., Kumar, A., and Herbein, G. (2015). The eEF1A proteins: at the crossroads of oncogenesis, apoptosis, and viral infections. Front. Oncol. *5*, 75.

Alexander, P.A., He, Y., Chen, Y., Orban, J., and Bryan, P.N. (2007). The design and characterization of two proteins with 88% sequence identity but different structure and function. Proc. Natl. Acad. Sci. USA *104*, 11963–11968.

Alexander, P.A., He, Y., Chen, Y., Orban, J., and Bryan, P.N. (2009). A minimal sequence code for switching protein structure and function. Proc. Natl. Acad. Sci. USA *106*, 21149–21154.

Amiri, A., Noei, F., Jeganathan, S., Kulkarni, G., Pinke, D.E., and Lee, J.M. (2007). eEF1A2 activates Akt and stimulates Akt-dependent actin remodeling, invasion and migration. Oncogene *26*, 3027–3040.

Anand, N., Murthy, S., Amann, G., Wernick, M., Porter, L.A., Cukier, I.H., Collins, C., Gray, J.W., Diebold, J., Demetrick, D.J., et al. (2002). Protein elongation factor EEF1A2 is a putative oncogene in ovarian cancer. Nat. Genet. *31*, 301–305.

Andersen, G.R., Pedersen, L., Valente, L., Chatterjee, I., Kinzy, T.G., Kjeldgaard, M., and Nyborg, J. (2000). Structural basis for nucleotide exchange and competition with tRNA in the yeast elongation factor complex eEF1A:eEF1Bα. Mol. Cell *6*, 1261–1266.

Bai, S.W., Herrera-Abreu, M.T., Rohn, J.L., Racine, V., Tajadura, V., Suryavanshi, N., Bechtel, S., Wiemann, S., Baum, B., and Ridley, A.J. (2011). Identification and characterization of a set of conserved and new regulators of cytoskeletal organization, cell morphology and migration. BMC Biol. *9*, 54.

Budkevich, T.V., Timchenko, A.A., Tiktopulo, E.I., Negrutskii, B.S., Shalak, V.F., Petrushenko, Z.M., Aksenov, V.L., Willumeit, R., Kohlbrecher, J., Serdyuk, I.N., et al. (2002). Extended conformation of mammalian translation elongation factor 1A in solution. Biochemistry *41*, 15342–15349.

Bunai, F., Ando, K., Ueno, H., and Numata, O. (2006). Tetrahymena eukaryotic translation elongation factor 1A (eEF1A) bundles filamentous actin through dimer formation. J. Biochem. *140*, 393–399.

Cao, H., Zhu, Q., Huang, J., Li, B., Zhang, S., Yao, W., and Zhang, Y. (2009). Regulation and functional role of eEF1A2 in pancreatic carcinoma. Biochem. Biophys. Res. Commun. *380*, 11–16.

Crepin, T., Shalak, V.F., Yaremchuk, A.D., Vlasenko, D.O., McCarthy, A., Negrutskii, B.S., Tukalo, M.A., and El'skaya, A.V. (2014). Mammalian translation elongation factor eEF1A2: X-ray structure and new features of GDP/GTP exchange mechanism in higher eukaryotes. Nucleic Acids Res. *42*, 12939–12948.

de Wit, N.J.W., Burtscher, H.J., Weidle, U.H., Ruiter, D.J., and van Muijen, G.N.P. (2002). Differentially expressed genes identified in human melanoma cell lines with different metastatic behaviour using high density oligonucleotide arrays. Melanoma Res. *12*, 57–69.

Doyle, A., Crosby, S.R., Burton, D.R., Lilley, F., and Murphy, M.F. (2011). Actin bundling and polymerisation properties of eukaryotic elongation factor 1α (eEF1A), histone H2A-H2B and lysozyme *in vitro*. J. Struct. Biol. *176*, 370–378.

Durso, N.A. and Cyr, R.J. (1994). A calmodulin-sensitive interaction between microtubules and a higher plant homolog of elongation factor-1α. Plant Cell *6*, 893–905.

Ejiri, S. (2002). Moonlighting functions of polypeptide elongation factor 1: from actin bundling to zinc finger protein R1-associated nuclear localization. Biosci. Biotechnol. Biochem. *66*, 1–21.

El'skaya, A.V., Negrutskii, B.S., Shalak, V.F., Vislovukh, A.A., Vlasenko, D.O., Novosylna, A.V., Lukash, T.O., and Veremieva, M.V. (2013). Specific features of protein biosynthesis in higher eukaryotes. Biopolym. Cell. *29*, 177–187.

Fife, C.M., McCarroll, J.A., and Kavallaris, M. (2014). Movers and shakers: cell cytoskeleton in cancer metastasis. Br. J. Pharmacol. *171*, 5507–5523.

Fu, W., Sun, J., Huang, G., Liu, J.C., Kaufman, A., Ryan, R.J.H., Ramanathan, S.Y., Venkatesh, T., and Singh, B. (2016).

Squamous cell carcinoma-related oncogene (SCCRO) family members regulate cell growth and proliferation through their cooperative and antagonistic effects on cullin neddylation. J. Biol. Chem. *291*, 6200–6217.

Fujimoto, H. and Mabuchi, I. (2010). Elongation factors are involved in cytokinesis of sea urchin eggs. Genes Cells *15*, 123–135.

Gross, S.R. and Kinzy, T.G. (2005). Translation elongation factor 1A is essential for regulation of the actin cytoskeleton and cell morphology. Nat. Struct. Mol. Biol. *12*, 772–778.

Guo, X., Wang, L., Li, J., Ding, Z., Xiao, J., Yin, X., He, S., Shi, P., Dong, L., Li, G., et al. (2015). Structural insight into autoinhibition and histone H3-induced activation of DNMT3A. Nature *517*, 640–644.

Hashimoto, Y., Parsons, M., and Adams, J.C. (2007). Dual actin-bundling and protein kinase C-binding activities of fascin regulate carcinoma cell migration downstream of Rac and contribute to metastasis. Mol. Biol. Cell *18*, 4591–4602.

Huang, G., Stock, C., Bommelje, C.C., Weeda, V.B., Shah, K., Bains, S., Buss, E., Shaha, M., Rechler, W., Ramanathan, S.Y., et al. (2014). SCCRO3 (DCUN1D3) antagonizes the neddylation and oncogenic activity of SCCRO (DCUN1D1). J. Biol. Chem. *289*, 34728–34742.

Jacobsen, K.T., Adlerz, L., Multhaup, G., and Iverfeldt, K. (2010). Insulin-like growth factor-1 (IGF-1)-induced processing of amyloid-beta precursor protein (APP) and APP-like protein 2 is mediated by different metalloproteinases. J. Biol. Chem. *285*, 10223–10231.

Kanibolotsky, D.S., Novosyl'na, O.V., Abbott, C.M., Negrutskii, B.S., and El'skaya, A.V. (2008). Multiple molecular dynamics simulation of the isoforms of human translation elongation factor 1A reveals reversible fluctuations between "open" and "closed" conformations and suggests specific for eEF1A1 affinity for $Ca^{2+}$-calmodulin. BMC Struct. Biol. *8*, 4.

Kaur, K.J. and Ruben, L. (1994). Protein translation elongation factor-1α from *Trypanosoma brucei* binds calmodulin. J. Biol. Chem. *269*, 23045–23050.

Kawamura, M., Endo, C., Sakurada, A., Hoshi, F., Notsuda, H., and Kondo, T. (2014). The prognostic significance of eukaryotic elongation factor 1 α-2 in non-small cell lung cancer. Anticancer Res. *34*, 651–658.

Khan, D.H., He, S., Yu, J., Winter, S., Cao, W., Seiser, C., and Davie, J.R. (2013). Protein kinase CK2 regulates the dimerization of histone deacetylase 1 (HDAC1) and HDAC2 during mitosis. J. Biol. Chem. *288*, 16518–16528.

Kim, Y., Roh, S., Park, J.-Y., Kim, Y., Cho, D.H., and Kim, J.C. (2009). Differential expression of the LOX family genes in human colorectal adenocarcinomas. Oncol. Rep. *22*, 799–804.

Knudsen, S.M., Frydenberg, J., Clark, B.F., and Leffers, H. (1993). Tissue-dependent variation in the expression of elongation factor-1α isoforms: isolation and characterisation of a cDNA encoding a novel variant of human elongation-factor 1α. Eur. J. Biochem. *215*, 549–554.

Kurasawa, Y., Hanyu, K., Watanabe, Y., and Numata, O. (1996). F-actin bundling activity of *Tetrahymena* elongation factor 1α is regulated by $Ca^{2+}$/calmodulin. J. Biochem. *119*, 791–798.

Laemmli, U.K. (1970). Cleavage of structural proteins during the assembly of the head of bacteriophage T4. Nature *227*, 680–685.

Lamberti, A., Caraglia, M., Longo, O., Marra, M., Abbruzzese, A., and Arcari, P. (2004). The translation elongation factor 1A in tumorigenesis, signal transduction and apoptosis: review article. Amino Acids *26*, 443–448.

Lau, A.W., Fukushima, H., and Wei, W. (2012). The Fbw7 and βTRCP E3 ubiquitin ligases and their roles in tumorigenesis. Front. Biosci. (Landmark Ed.), *17*, 2197–2212.

Lee, J.M. (2003). The role of protein elongation factor eEF1A2 in ovarian cancer. Reprod. Biol. Endocrinol. *1*, 69.

Lee, M.-H. and Surh, Y.-J. (2009). eEF1A2 as a putative oncogene. Ann. N.Y. Acad. Sci. *1171*, 87–93.

Lee, S., Wolfraim, L.A., and Wang, E. (1993). Differential expression of S1 and elongation factor-1α during rat development. J. Biol. Chem. *268*, 24453–24459.

Li, R., Wang, H., Bekele, B.N., Yin, Z., Caraway, N.P., Katz, R.L., Stass, S.A., and Jiang, F. (2006). Identification of putative oncogenes in lung adenocarcinoma by a comprehensive functional genomic approach. Oncogene *25*, 2628–2635.

Lukash, T.O., Turkivska, H.V., Negrutskii, B.S., and El'skaya, A.V. (2004). Chaperone-like activity of mammalian elongation factor eEF1A: renaturation of aminoacyl-tRNA synthetases. J. Biochem. Cell Biol. *36*, 1341–1347.

Migliaccio, N., Ruggiero, I., Martucci, N.M., Sanges, C., Arbucci, S., Tate, R., Rippa, E., Arcari, P., and Lamberti, A. (2015). New insights on the interaction between the isoforms 1 and 2 of human translation elongation factor 1A. Biochimie *118*, 1–7.

Mohler, J.L., Morris, T.L., Ford, O.H. 3rd, Alvey, R.F., Sakamoto, C., and Gregory, C.W. (2002). Identification of differentially expressed genes associated with androgen-independent growth of prostate cancer. Prostate *51*, 247–255.

Moore, R.C., Durso, N.A., and Cyr, R.J. (1998). Elongation factor-1alpha stabilizes microtubules in a calcium/calmodulin-dependent manner. Cell Motil. Cytoskeleton *41*, 168–180.

Morita, K., Bunai, F., and Numata, O. (2008). Roles of three domains of tetrahymena eEF1A in bundling F-actin. Zoolog. Sci. *25*, 22–29.

Mouneimne, G., Hansen, S.D., Selfors, L.M., Petrak, L., Hickey, M.M., Gallegos, L.L., Simpson, K.J., Lim, J., Gertler, F.B., Hartwig, J.H., et al. (2012). Differential remodeling of actin cytoskeleton architecture by profilin isoforms leads to distinct effects on cell migration and invasion. Cancer Cell *22*, 615–630.

Negrutskii, B.S. and El'skaya, A.V. (1998). Eukaryotic translation elongation factor 1 alpha: structure, expression, functions, and possible role in aminoacyl-tRNA channeling. Prog. Nucleic Acid Res. Mol. Biol. *60*, 47–78.

Negrutskii, B., Vlasenko, D., and El'skaya, A. (2012). From global phosphoproteomics to individual proteins: the case of translation elongation factor eEF1A. Expert Rev. Proteomics *9*, 71–83.

Newbery, H.J., Loh, D.H., O'Donoghue, J.E., Tomlinson, V.A.L., Chau, Y.-Y., Boyd, J.A., Bergmann, J.H., Brownstein, D., and Abbott, C.M. (2007). Translation elongation factor eEF1A2 is essential for post-weaning survival in mice. J. Biol. Chem. *282*, 28951–28959.

Nissen, P., Thirup, S., Kjeldgaard, M., and Nyborg, J. (1999). The crystal structure of Cys-tRNACys-EF-Tu-GDPNP reveals general and specific features in the ternary complex and in tRNA. Structure *7*, 143–156.

Novosylna, O.V., Timchenko, A.A., Tiktopulo, E.I., Serdyuk, I.N., Negrutskii, B.S., and El'skaya, A.V. (2007). Characterization of physical properties of two isoforms of translation elongation factor 1A. Biopolym. Cell *23*, 386–390.

Novosylna, O., Jurewicz, E., Pydiura, N., Goral, A., Filipek, A., Negrutskii, B., and El'skaya, A. (2015). Translation elongation factor eEF1A1 is a novel partner of a multifunctional protein Sgt1. Biochimie *119*, 137–145.

Palmer, S.R., Crowley, P.J., Oli, M.W., Ruelf, M.A., Michalek, S.M., and Brady, L.J. (2012). YidC1 and YidC2 are functionally distinct proteins involved in protein secretion, biofilm formation and cariogenicity of Streptococcus mutans. Microbiology *158*, 1702–1712.

Panasyuk, G., Nemazanyy, I., Filonenko, V., Negrutskii, B., and El'skaya, A.V. (2008). A2 isoform of mammalian translation factor eEF1A displays increased tyrosine phosphorylation and ability to interact with different signalling molecules. J. Biochem. Cell Biol. *40*, 63–71.

Pettersen, E.F., Goddard, T.D., Huang, C.C., Couch, G.S., Greenblatt, D.M., Meng, E.C., and Ferrin, T.E. (2004). UCSF Chimera – a visualization system for exploratory research and analysis. J. Comput. Chem. *25*, 1605–1612.

Rao, J. and Li, N. (2004). Microfilament actin remodeling as a potential target for cancer drug development. Curr. Cancer Drug Targets *4*, 345–354.

Sali, A. and Blundell, T.L. (1993). Comparative protein modelling by satisfaction of spatial restraints. J. Mol. Biol. *234*, 779–815.

Samyesudhas, S.J., Roy, L., and Cowden Dahl, K.D. (2014). Differential expression of ARID3B in normal adult tissue and carcinomas. Gene *543*, 174–180.

Sasikumar, A.N., Perez, W.B., and Kinzy, T.G. (2012). The many roles of the eukaryotic elongation factor 1 complex. Wiley Interdiscip. Rev. RNA *3*, 543–555.

Scaggiante, B. and Bosutti, A. (2015). EEF1A1 (eukaryotic translation elongation factor 1 alpha 1). Atlas Genet. Cytogenet. Oncol. Haematol. *19*, 256–265.

Sengprasert, P., Amparyup, P., Tassanakajorn, A., and Wongpanya, R. (2015). Characterization and identification of calmodulin and calmodulin binding proteins in hemocyte of the black tiger shrimp (*Penaeus monodon*). Dev. Comp. Immunol. *50*, 87–97.

Shalak, V.F., Budkevich, T.V., Negrutskil, B.S., and El'skaia, A.V. (1997). A fast and effective method for purification of elongation factor 1$\alpha$ from rabbit liver. Ukr. Biochem. J. *69*, 104–109.

Shiau, A.K., Harris, S.F., Southworth, D.R., and Agard, D.A. (2006). Structural analysis of *E. coli* hsp90 reveals dramatic nucleotide-dependent conformational rearrangements. Cell *127*, 329–340.

Sirianant, L., Ousingsawat, J., Tian, Y., Schreiber, R., and Kunzelmann, K. (2014). TMC8 (EVER2) attenuates intracellular signaling by $Zn^{2+}$ and $Ca^{2+}$ and suppresses activation of $Cl^-$ currents. Cell. Signal. *26*, 2826–2833.

Soares, D.C., Barlow, P.N., Newbery, H.J., Porteous, D.J., and Abbott, C.M. (2009). Structural models of human eEF1A1 and eEF1A2 reveal two distinct surface clusters of sequence variation and potential differences in phosphorylation. PLoS One *4*, e6315.

Stevenson, R.P., Veltman, D., and Machesky, L.M. (2012). Actin-bundling proteins in cancer progression at a glance. J. Cell Sci. *125*, 1073–1079.

Sun, Y., Du, C., Wang, B., Zhang, Y., Liu, X., and Ren, G. (2014). Up-regulation of eEF1A2 promotes proliferation and inhibits apoptosis in prostate cancer. Biochem. Biophys. Res. Commun. *450*, 1–6.

Timchenko, A.A., Novosylna, O.V., Prituzhalov, E.A., Kihara, H., El'skaya, A.V., Negrutskii, B.S., and Serdyuk, I.N. (2013). Different oligomeric properties and stability of highly homologous A1 and proto-oncogenic A2 variants of mammalian translation elongation factor eEF1. Biochemistry *52*, 5345–5353.

Tomlinson, V.A.L., Newbery, H.J., Wray, N.R., Jackson, J., Larionov, A., Miller, W.R., Dixon, J.M., and Abbott, C.M. (2005). Translation elongation factor eEF1A2 is a potential oncoprotein that is overexpressed in two-thirds of breast tumours. BMC Cancer. *5*, 113.

Tossidou, I., Niedenthal, R., Klaus, M., Teng, B., Worthmann, K., King, B.L., Peterson, K.J., Haller, H., and Schiffer, M. (2012). CD2AP regulates SUMOylation of CIN85 in podocytes. Mol. Cell. Biol. *32*, 1068–1079.

Vislovukh, A., Kratassiouk, G., Porto, E., Gralievska, N., Beldiman, C., Pinna, G., El'skaya, A., Harel-Bellan, A., Negrutskii, B., and Groisman, I. (2013). Proto-oncogenic isoform A2 of eukaryotic translation elongation factor eEF1 is a target of miR-663 and miR-744. Br. J. Cancer *108*, 2304–11.

Vlasenko, D.O., Novosylna, O.V., Negrutskii, B.S., and Anna, V. (2015). Truncation of the A, A∗, A′ helices segment impairs the actin bundling activity of mammalian eEF1A1. FEBS Lett. *589*, 1187–1193.

Wanitchakool, P., Wolf, L., Koehl, G.E., Sirianant, L., Schreiber, R., Kulkarni, S., Duvvuri, U., and Kunzelmann, K. (2014). Role of anoctamins in cancer and apoptosis. Philos. Trans. R. Soc. Lond. B. Biol. Sci. *369*, 20130096.

Werner, A., Iwasaki, S., McGourty, C.A., Medina-Ruiz, S., Teerikorpi, N., Fedrigo, I., Ingolia, N.T., and Rape, M. (2015). Cell-fate determination by ubiquitin-dependent regulation of translation. Natur *525*, 523–527.

Xie, D., Jauch, A., Miller, C.W., Bartram, C.R., and Koeffler, H.P. (2002). Discovery of over-expressed genes and genetic alterations in breast cancer cells using a combination of suppression subtractive hybridization, multiplex FISH and comparative genomic hybridization. Int. J. Oncol. *21*, 499–507.

Xu, C., Hu, D., and Zhu, Q. (2013). eEF1A2 promotes cell migration, invasion and metastasis in pancreatic cancer by upregulating MMP-9 expression through Akt activation. Clin. Exp. Metastasis *30*, 933–944.

Yang, S., Lu, M., Chen, Y., Meng, D., Sun, R., Yun, D., Zhao, Z., Lu, D., and Li, Y. (2015). Overexpression of eukaryotic elongation factor 1 alpha-2 is associated with poorer prognosis in patients with gastric cancer. J. Cancer Res. Clin. Oncol. *141*, 1265–1275.

Yap, K.L., Kim, J., Truong, K., Sherman, M., Yuan, T., and Ikura, M. (2000). Calmodulin target database. J. Struct. Funct. Genomics. *1*, 8–14.

Yaremchuk, A., Shalak, V.F., Novosylna, O.V., Negrutskii, B.S., Crepin, T., El'skaya, A.V., and Tukalo, M. (2012). Purification, crystallization and preliminary X-ray crystallographic analysis of mammalian translation elongation factor eEF1A2. Acta Crystallogr. Sect. F Struct. Biol. Cryst. Commun. *68*, 295–297.

Zhu, H., Lam, D.C.L., Han, K.C., Tin, V.P.C., Suen, W.S., Wang, E., Lam, W.K., Cai, W.W., Chung, L.P., and Wong, M.P. (2007). High resolution analysis of genomic aberrations by metaphase and array comparative genomic hybridization identifies candidate tumour genes in lung cancer cell lines. Cancer Lett. *245*, 303–314.

**Supplemental Material:** The online version of this article (DOI: 10.1515/hsz-2016-0172) offers supplementary material, available to authorized users.